CHAPTER-V

Calculation of dipolar fields near the surface

5.1 Introduction

The local, or effective electric field for a polarisable infinite lattice has been studied for a long time (see for example, Born and Wolf[46]). Nijboer & Wette[47] (1958) evaluated the dipole field for both the cubic and non cubic (tetragonal, hexagonal, orthorhombic and monoclinic) lattices. They have considered a slab of dielectric material and obtained the dipole field by plane-wise summation. Using the same plane-wise summation method Kar & Bagchi[48](1978) calculated the dipole moment and the self-consistent local field near the surface of some cubic lattices. In this chapter, we consider three other structures, simple hexagonal, hexagonal close-packed (hcp) and diamond structure. The first two do not belong to the cubic system and so the Lorentz-Lorenz relation is not expected to hold (although, for the ideal hcp structure, the relation does hold); the Bravais lattice for the diamond structure is face-centred cubic, but the fact that there exists a two atom basis means that in addition to the atomic sites for the face-centred cubic structure there would be an equal number of atoms in other sites and the local field in the surface plane is quite different from the face-centred cubic case, as we shall discuss later.

The procedure for calculating the self-consistent local field is essentially the same as in ref 48; we have also used similar notations. A slab geometry of finite number of lattice plane have been considered - the lattice planes are assumed to be infinite, parallel to the surface. We have considered an electric field normal to the surface plane; the polarizability tensor was assumed to be diagonal; the molecules in each site would be polarised - these were taken as point dipoles - and all the dipoles lying in one plane would be parallel to one another and would have the same magnitude. The first step is to

compute the field from an infinite two-dimensional lattice of parallel dipoles of equal moment. This can be evaluated either by explicit sum within a finite region and approximating the rest by an integration with uniform dipole density[49] or by transforming the discrete lattice sum to a highly convergent sum analytically[47,50,51]. We have used the former technique to evaluate the two dimensional lattice sum. A major part of this work has already been published[52].

Let us denote different planes by the index ν and take $\vec{P}_\nu$ to be the local dipole moment density for the lattice plane ν. We shall consider $\nu=0$ to be the reference plane - positive values of ν denote planes with a positive value of z (above the reference plane) and negative ν values refer to planes below the reference plane. We shall consider an applied field $\vec{E}_0 = E_0\hat{z}$ in the z- direction. The field from the dipoles in the plane ν will depend linearly on $\vec{P}_\nu$ and the z-component of the total contribution of all the dipole fields may be written as

$$E_{d,z} = \sum_\nu \xi_\nu P_\nu \qquad (5.1)$$

where the sum over ν includes in principle all the planes in the slab we are considering and the coefficient ξ_ν has to be determined for each lattice structure. However, only a few of the ξ_ν's have non-zero values - at least to the accuracy we are concerned with.

We now consider a slab of L lattice planes. The local electric field at a lattice point in the μ-th plane, (μ=1,2, . . . L) may be written as

$$E^{\mu}_{loc,z} = E_0 + \sum_{\nu} \xi_{\mu-\nu} P_{\nu}$$

(5.2)

where the sum over ν is from 1 to L (although, in practice, only those terms for which ξ's are non-zero have to be retained).

Taking the volume polarisabilty to be Γ, the self-consistency condition for the local dipole moment density, given below

$$P_{\mu} = \Gamma E^{\mu}_{loc,z}$$

will yield the matrix equation

$$\sum_{\nu} M_{\mu\nu} P_{\nu} = \Gamma E_0 , \qquad \mu = 1, 2, \ldots L$$

$$\text{where } M_{\mu\nu} = \left[(1 - \Gamma\xi_0)\,\delta_{\mu\nu} - \Gamma\xi_{\mu-\nu}(1-\delta_{\mu\nu}) \right]$$

(5.3)

Inversion of the matrix M, where it is permissible, gives us the self-consistent dipole moment density on each plane; in particular, it would give the behaviour near the surface. Then, by using formula (5.2) we can compute the dipolar field on each plane.

In the following we shall consider the three structures - simple hexagonal, hexagonal close-packed and diamond, separately. In each case we shall give expressions for ξ and compute the self-consistent dipole moment and the dipolar field plane by plane. We shall also discuss the significance of the results obtained.

5.2 SIMPLE HEXAGONAL STRUCTURE

In fig. 5.1 we have shown a hexagonal close-packed structure where, the zero'th plane and the second (even) planes are the same for the simple hexagonal structure. For the simple hexagonal lattice, the sites in a plane with reference to an origin at a lattice point may be written as

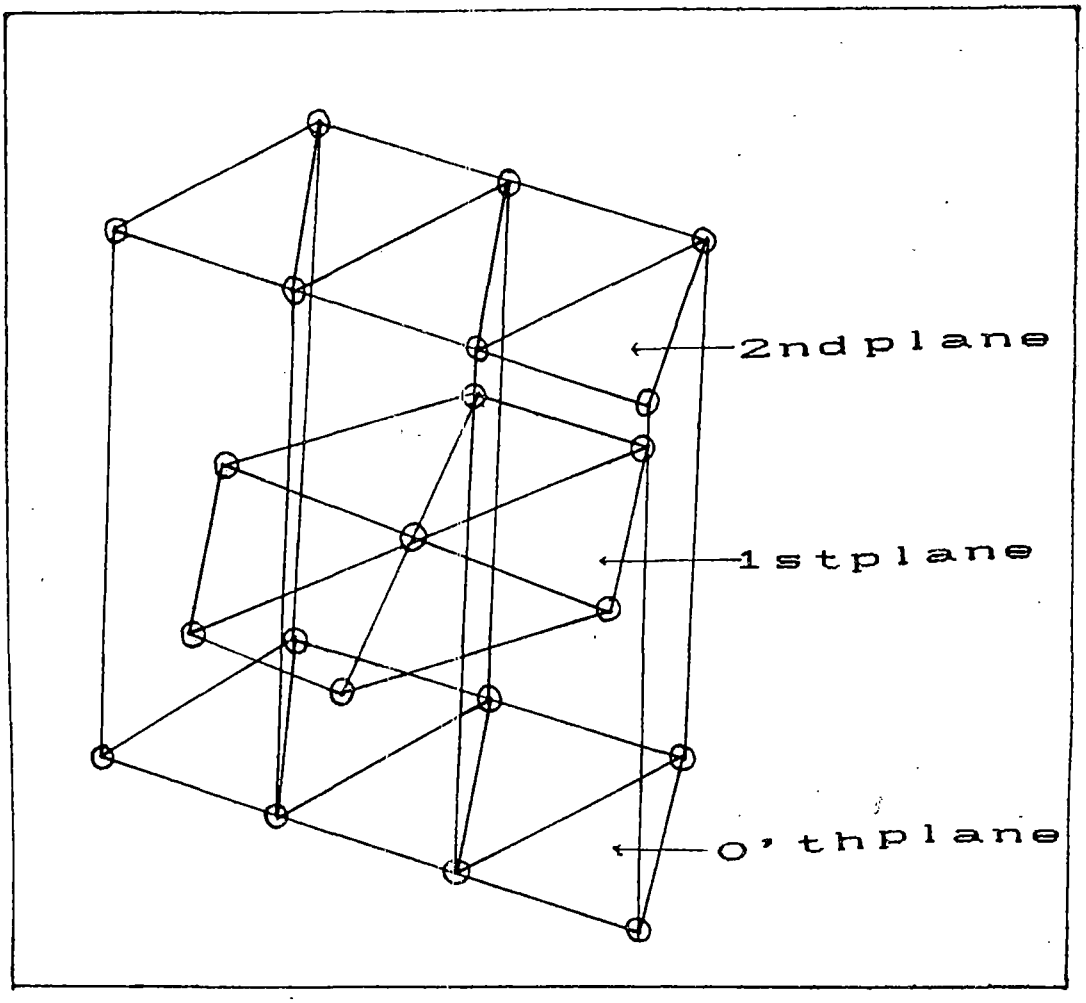

Fig 5.1 Schematic representation of hexagonal close-packed structure

$$\vec{R} = a\left[(n_1+\frac{n_2}{2})\hat{x}+\frac{\sqrt{3}}{2}n_2\hat{y}\right]$$

and for any other plane parallel to it, we may write

$$\vec{R} = a\left[(n_1+\frac{n_2}{2})\hat{x}+\frac{\sqrt{3}}{2}n_2\hat{y}+\alpha n_3\hat{z}\right]$$

where α=c/a and the surface is taken to be perpendicular to the z-axis. The electric field due to a dipole of moment $\vec{d}_i$ at point $\vec{r}_i$ is

$$\vec{E}_d=\sum_i' \frac{3(\vec{d}_i.\vec{r}_i).\vec{r}_i-r_i^2\vec{d}_i}{r_i^5}$$

(5.4)

If we consider $\vec{r}_i$ as the lattice vectors in the reference plane and noting that if $\vec{d}_\mu$ is the dipole moment for the dipole in the plane μ, then the dipole moment density for that plane $\vec{P}_\mu$ is

$$\vec{P}_\mu = \frac{2\vec{d}_\mu}{\sqrt{3}\alpha a^3}$$

Using equation (5.1 & 5.4) we can obtain the expression for ξ_0 as

$$\xi_0 = -(\frac{\sqrt{3}}{2}\alpha)\sum'_{n_1,n_2}\frac{1}{\left[n_1^2+n_2^2+n_1n_2\right]^{\frac{3}{2}}}$$

(5.5)

(the point $n_1=n_2=0$ is excluded)

Similarly, for the other planes we note that $\xi_\mu=\xi_{-\mu}$ and

$$\xi_\mu = (\frac{\sqrt{3}}{2}\alpha)\sum_{n_1,n_2}\frac{3n_3^2\alpha^2-\left[n_1^2+n_2^2+n_1n_2+\alpha^2n_3^2\right]}{\left[n_1^2+n_2^2+n_1n_2+\alpha^2n_3^2\right]^{\frac{5}{2}}}$$

(5.6)

with the plane index $\mu=n_3$, $n_3=1, 2, \ldots$ etc. The values of ξ_0, ξ_1, etc. calculated from equation (5.5-6) are shown in Table 1 for

Table 1: ξ_μ for various planes for simple hexagonal, hcp and diamond structure.

Plane Index μ	ξ_μ			
	Hexagonal	Hexagonal Close-Packed		Diamond
	a = 1.59	a = 1.63	a = 1.86	
0	-15.6046	-7.8023	-7.8023	-3.1939
1	0.0043	-0.2868	-0.1460	-2.0862
2	0.0000	0.0015	0.0003	-0.5054
3	0.0000	0.0006	0.0000	-0.0062
4	0.0000	0.0000	0.0000	0.0080
5	0.0000	0.0000	0.0000	0.0000

$a=1.59$ (this value is typical of simple hexagonal structures). These are in agreement with the previously computed values[47,51]. Further, to the accuracy we are interested in, it is necessary to take only ξ_0 and ξ_1 into account - so the sum in equation(5.2) would be restricted to $|\mu - \nu| \leq 1$.

We have also calculated[52] P_μ/P_b and E_μ/E_b (where P_b and E_b are the bulk values of the dipole moment and the dipole field) for a 21- layer film with a number of values of the volume polarizability Γ. In figure 5.2, we have plotted E_μ/E_b and P_μ/P_b for $\Gamma = -0.1$, but there is virtually no change if we take any other value of Γ. We have seen that 21 layers are enough to ensure convergence; actually, in this case convergence may be achieved even with a fewer number of layers. Except for a very small range near $\Gamma = -0.064$ for which the matrix cannot be inverted, the results look the same - with virtually no change at the surface plane for the dipole moment or the dipolar field. This is not unexpected - since we have seen that $|\xi_0/\xi_1| \sim 3.6\times10^3$, almost the entire contribution to the dipolar field comes from the in-plane dipoles - and so there is almost no variation in P_μ/P_b or E_μ/E_b from plane to plane.

5.3 HEXAGONAL CLOSE-PACKED STRUCTURE

For this structure, in addition to the lattice planes for the simple hexagonal case we have another set of planes halfway between the former ones as shown in Figure 5.1. The coefficient ξ_0 can be calculated using the same formula (5.5) as in the case of simple hexagonal structure, with an additional factor of 1/2 which comes in as there are now two atoms per unit cell. The original planes of the simple hexagonal lattice now become even numbered planes, and we may use equation (5.6) to calculate ξ_μ, with an additional factor of 1/2 with $\mu=2n_z$. For the odd-numbered planes we note that the sites may be denoted

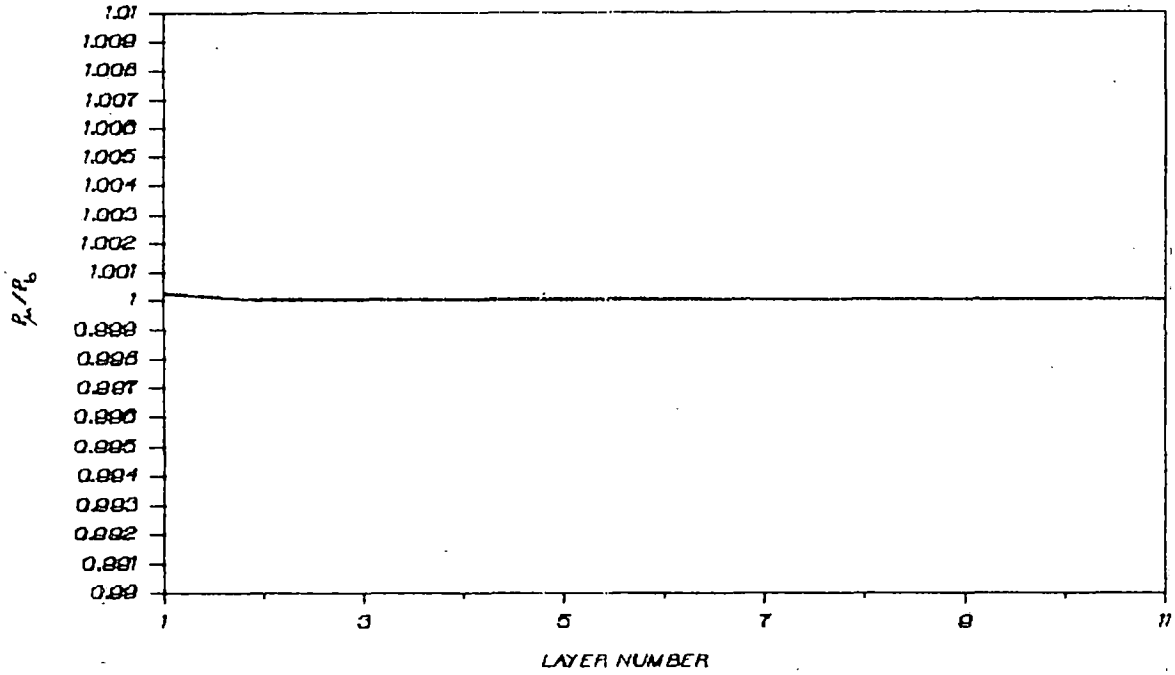

[a]

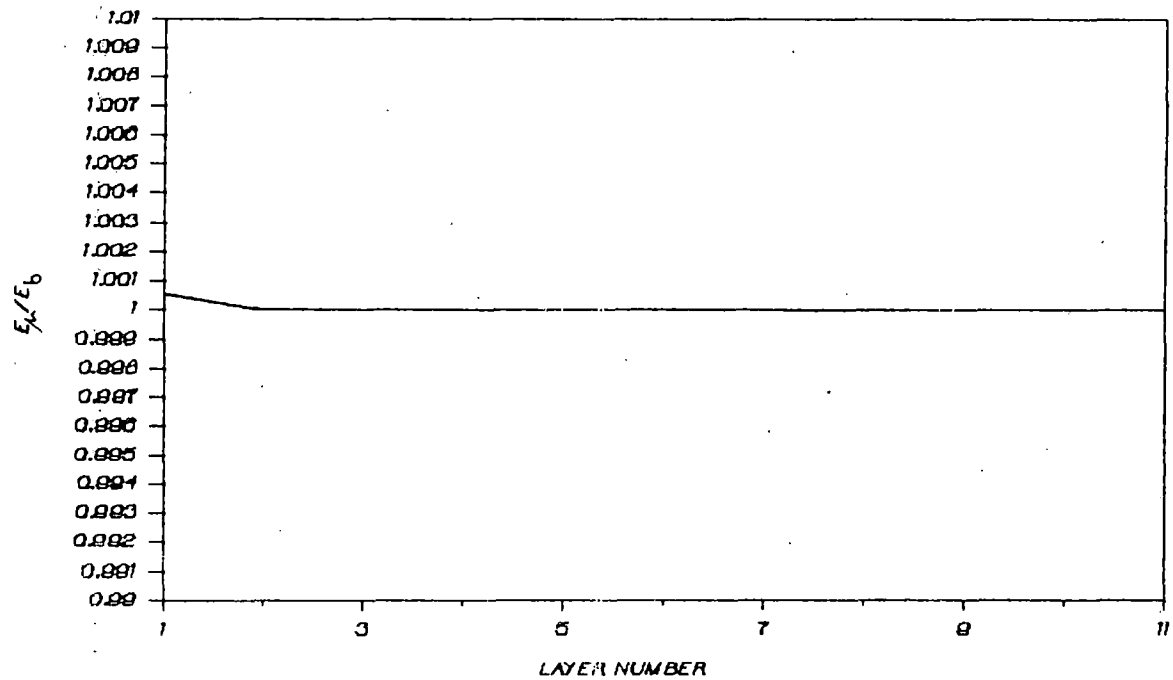

[b]

Fig 5.2 Variation of [a] ($P\mu/P_b$) and [b] ($E\mu/E_b$) against μ for Γ =-0.1 in simple hexagonal lattice

by the vectors

$$\vec{R} = (n_1+\frac{1}{3})\vec{a}_1 + (n_2+\frac{1}{3})\vec{a}_2 + (n_3+\frac{1}{2})\vec{a}_3$$

$$\text{with} \quad \vec{a}_1 = a\hat{x}, \; \vec{a}_2 = \frac{1}{2}a\hat{x} + \frac{\sqrt{3}}{2}a\hat{y}, \; \vec{a}_3 = c\hat{z}$$

We can then write, for odd planes

$$\xi_\mu = \frac{\sqrt{3}}{4}\alpha \sum_{n_1,n_2} \frac{3\alpha^2(n_3+\frac{1}{2})^2 - \left[(n_1+\frac{n_2}{2}+\frac{1}{2})^2 + \frac{3}{4}(n_2+\frac{1}{3})^2 + \alpha^2(n_3+\frac{1}{2})^2\right]}{\left[(n_1+\frac{n_2}{2}+\frac{1}{2})^2 + \frac{3}{4}(n_2+\frac{1}{3})^2 + \alpha^2(n_3+\frac{1}{2})^2\right]^{\frac{5}{2}}}$$

(5.7)

with $\mu = 2n_3+1$

In Table 1, we have shown the computed values of ξ_μ obtained from equation (5.5-7) for two values of α, 1.63 (corresponding to IDEAL HCP structure) and 1.86. For cubic symmetry, it is known that

$$\sum_\mu \xi_\mu = -\frac{8\pi}{3}$$

which gives the familiar Lorentz-Lorenz result. We note that for the ideal HCP structure also, this relation holds - although the symmetry is not cubic. For α=1.86 however, the sum over ξ_μ does not give $-8\pi/3$. This is perhaps another illustration of the close relationship between the face-centred cubic and ideal hexagonal close-packed structure.

For determining the dipole moment and the dipolar field in the surface region, we have taken a 21 layer slab and constructed the matrix M in equation (5.3) and inverted it to obtain the dipole moments $\vec{P}_\mu$ and the dipolar field, layer by layer. It may be mentioned here that taking 21 layer ensures convergence and increasing the number of layers does not change P_μ/P_b or E_μ/E_b, at least to the accuracy we are interested

in. For α=1.63, in figure 5.3, we show P_μ/P_b and E_μ/E_b for three values of Γ. Actually the points for integral values of μ are relevant - these points have been joined by lines for visual aid. Γ =-0.10 and Γ =-0.14 correspond to values of Γ just beyond the range for which the matrix **M** may not be inverted. For Γ =-0.14. i.e. just below the forbidden range, we see the maximum enhancement in the dipolar field for the surface layer - although the enhancement is not very large. The behaviour for both E_μ/E_b and P_μ/P_b is both oscillatory for this value of Γ - again the similarity of behaviour with face-centred cubic case[48] may be noted. For Γ =-0.10, just above the forbidden range and Γ =0.1, the variation in the dipolar field for the surface layer is smaller and the oscillatory behaviour is also absent. For α=1.86, we have plotted (fig 5.4) P_μ/P_b and E_μ/E_b for the same three values of Γ - and the behaviour is qualitatively the same - but the difference between the surface and bulk values for E_μ (or P_μ) is smaller than for the ideal case.

5.4 DIAMOND STRUCTURE

The diamond structure has the face-centred cubic lattice as the underlying Bravais lattice with a two atom basis. In this case we have, therefore, in addition to FCC lattice planes, an equal number of planes interspaced between these as shown in fig 5.5. Here, the expression for dipole moment density would be

$$\vec{P}_\mu = \frac{8\vec{d}_\mu}{a^3}$$

and for the reference plane,

$$\vec{R} = \frac{a}{\sqrt{2}}(n_1\hat{i}+n_2\hat{j})$$

ξ_0 is given by

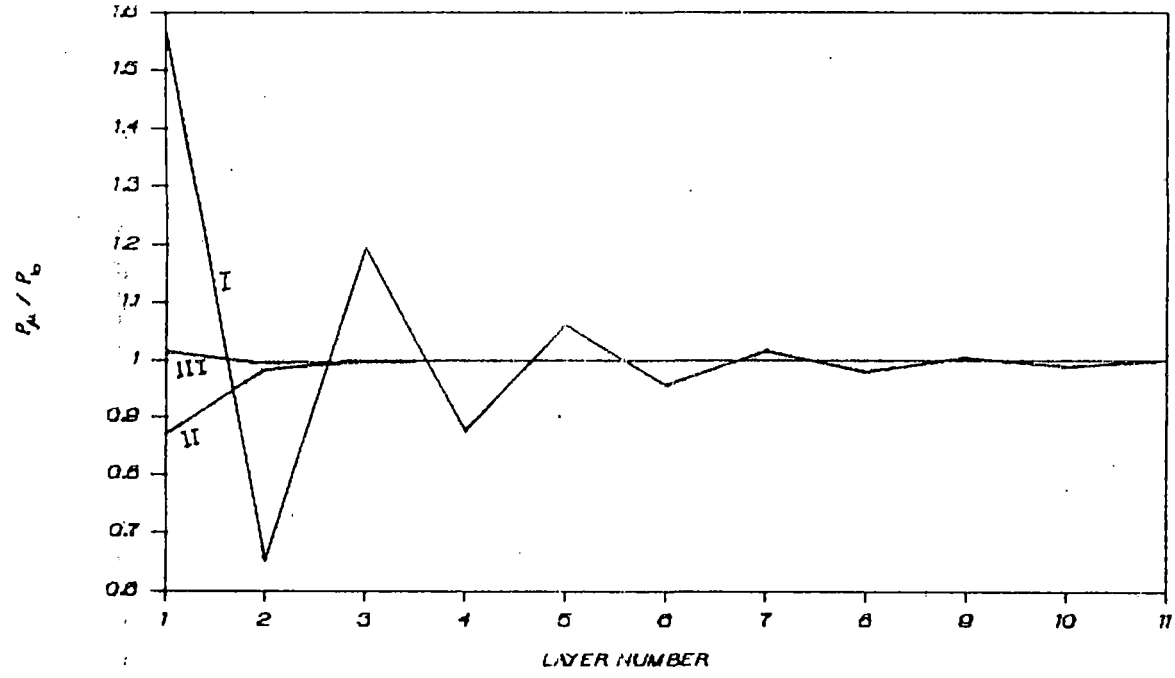

[a]

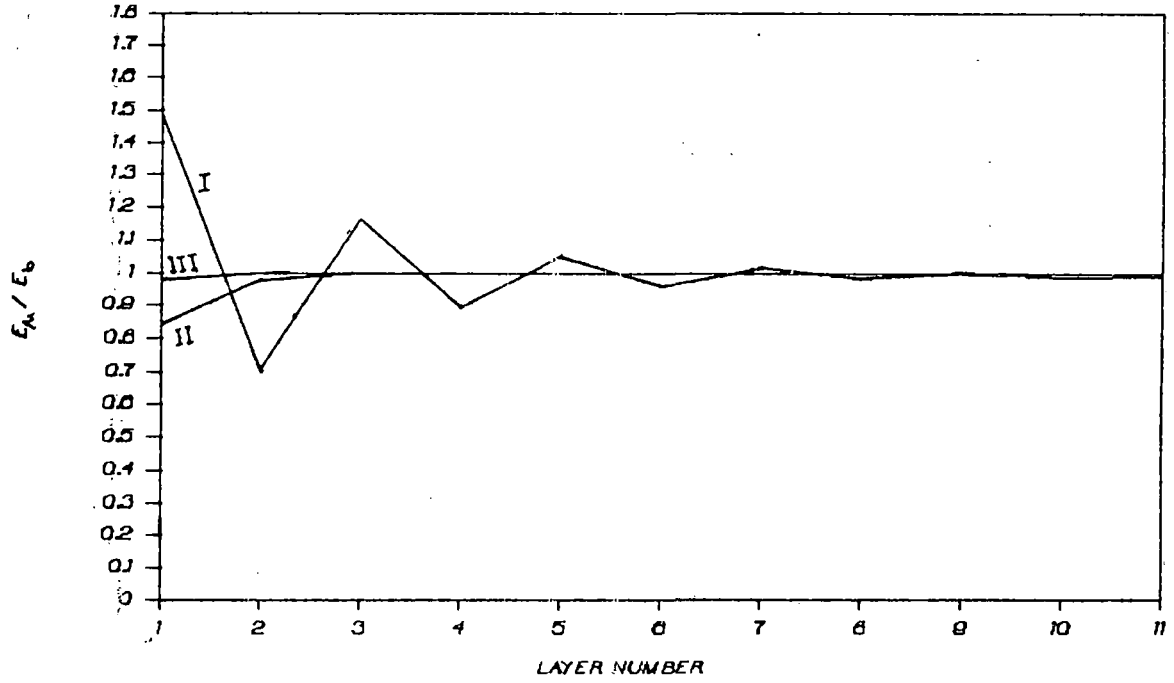

[b]

Fig 5.3 Variation of [a] $P\mu/P_b$ and [b] $E\mu/E_b$ against μ, for Γ =-0.14 (I), -0.1 (II) and 0.1 (III) in ideal hcp sturucture

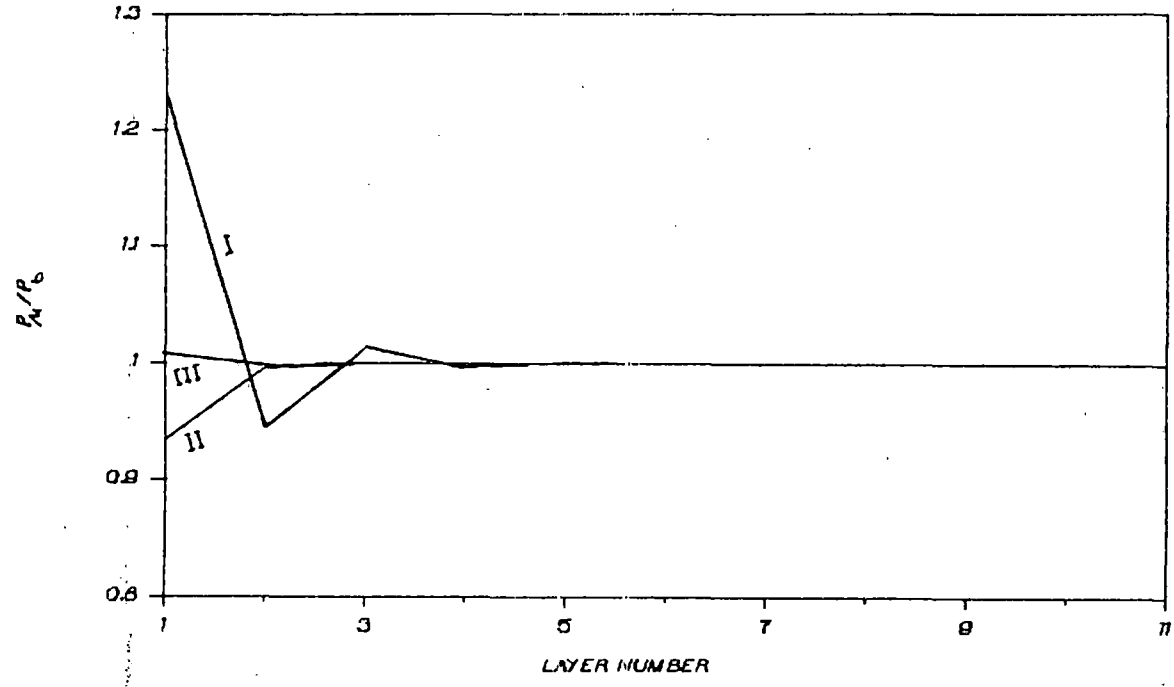

[a]

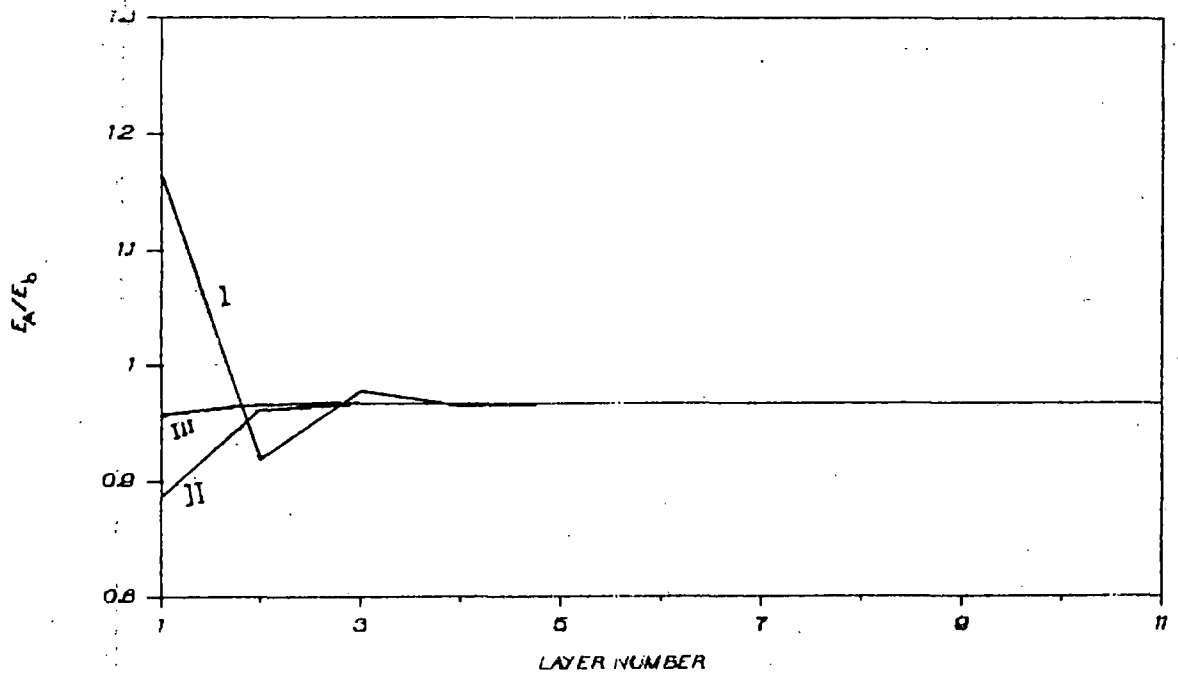

[b]

Fig 5.4 Variation of [a] $P\mu/P_b$ and [b] $E\mu/E_b$ against μ, for Γ =-0.14 (I), -0.1 (II) and 0.1 (III) in hcp structure with α=1.86

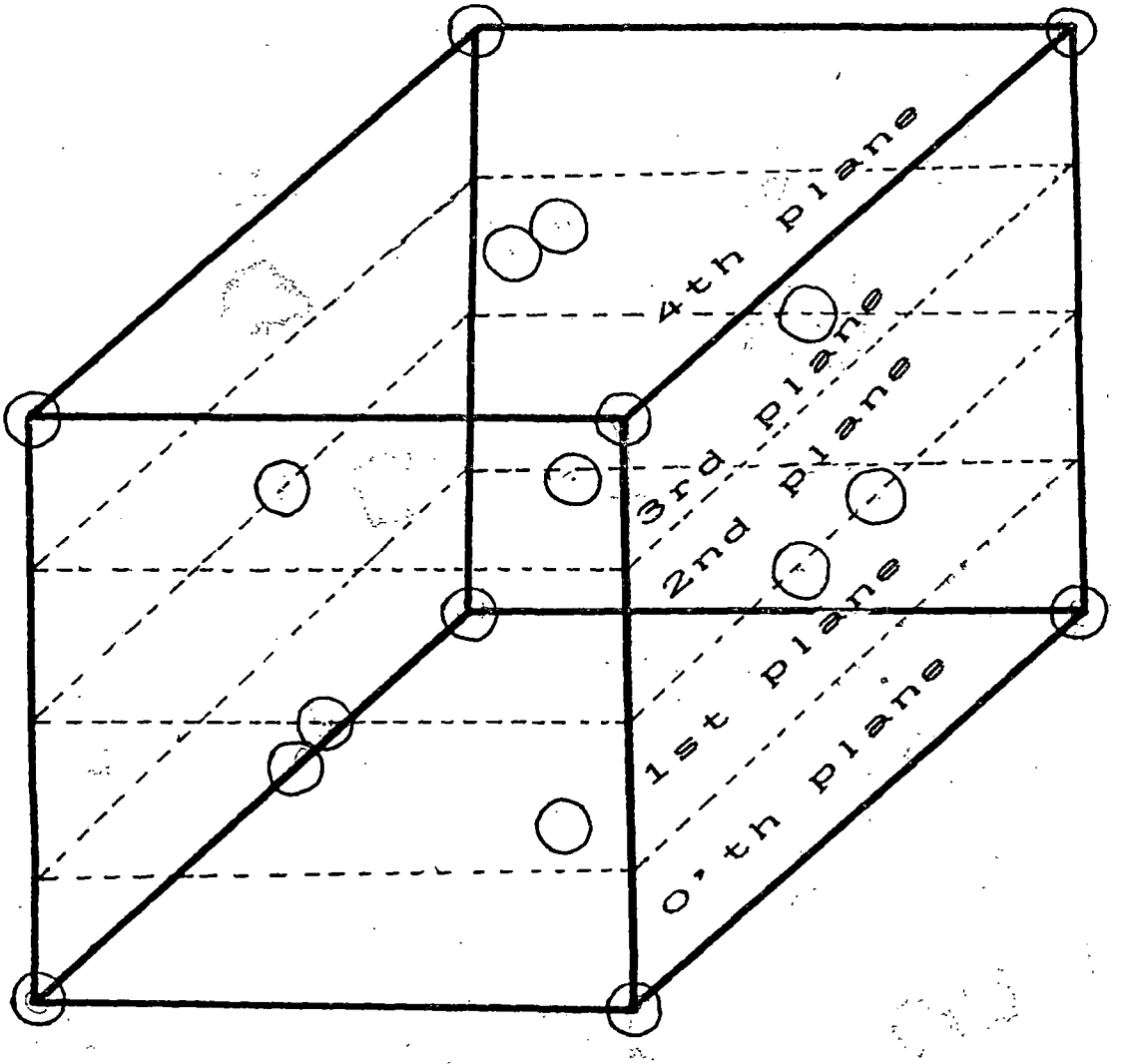

Fig 5.5 Schematic representation of diamond structure

$$\xi_0 = -\frac{1}{8}\sum\nolimits'_{n_1,n_2} \frac{1}{\left[\frac{1}{2}(n_1^2+n_2^2)\right]^{\frac{3}{2}}}$$

(5.8)

For planes located at distance (n+1/4)a from the reference plane (i,e. 1st plane, 5th plane etc.) i.e.,

$$\vec{R} = a\left[\frac{\hat{i}}{\sqrt{2}}n_1 + \frac{\hat{j}}{\sqrt{2}}(n_2+\frac{1}{2}) + \hat{k}(n_3+\frac{1}{4})\right]$$

we have

$$\xi_\mu = \frac{1}{8}\sum\nolimits_{n_1,n_2} \frac{3(n_3+\frac{1}{4})^2 - \left[\frac{n_1^2}{2} + \frac{1}{2}(n_2+\frac{1}{2})^2 + (n_3+\frac{1}{4})^2\right]}{\left[\frac{n_1^2}{2} + \frac{1}{2}(n_2+\frac{1}{2})^2 + (n_3+\frac{1}{4})^2\right]^{\frac{5}{2}}}$$

$$\text{with } \mu = 4n_3+1 \quad (n_3 = 0,1,2,\ldots)$$

(5.9)

For planes at distance (n+1/2)a from the reference plane (i.e. 2nd, 6th etc.) given by

$$\vec{R} = a\left[\frac{\hat{i}}{\sqrt{2}}(n_1+\frac{1}{2}) + \frac{\hat{j}}{\sqrt{2}}(n_2+\frac{1}{2}) + \hat{k}(n_3+\frac{1}{2})\right]$$

$$\xi_\mu = \frac{1}{8}\sum\nolimits_{n_1,n_2} \frac{3(n_3+\frac{1}{2})^2 - \left[\frac{1}{2}(n_1+\frac{1}{2})^2 + \frac{1}{2}(n_2+\frac{1}{2})^2 + (n_3+\frac{1}{2})^2\right]}{\left[\frac{1}{2}(n_1+\frac{1}{2})^2 + \frac{1}{2}(n_2+\frac{1}{2})^2 + (n_3+\frac{1}{2})^2\right]^{\frac{5}{2}}}$$

$$\text{with } \mu = 4n_3+2 \quad (n_3 = 0,1,2,..etc)$$

(5.10)

Similarly, for planes denoted by $\mu = 3,7,..$ etc

$$\vec{R} = a\left[\frac{\hat{i}}{\sqrt{2}}(n_1+\frac{1}{2}) + \frac{\hat{j}}{\sqrt{2}}(n_2+1) + \hat{k}(n_3+\frac{3}{4})\right]$$

$$\xi_\mu = \frac{1}{8}\sum_{n_1,n_2} \frac{3(n_3+\frac{3}{4})^2 - \left[\frac{1}{2}(n_1+\frac{1}{2})^2+\frac{1}{2}(n_2+1)^2+(\frac{3}{4}+n_3)^2\right]}{\left[\frac{1}{2}(n_1+\frac{1}{2})^2+\frac{1}{2}(n_2+1)^2+(\frac{3}{4}+n_3)^2\right]^{\frac{5}{2}}}$$

$$\text{with} \quad \mu = 4n_3+3 \quad (n_3 = 0,1,2,..)$$

(5.11)

and for planes denoted by $\mu=4,8$ ....etc.,

$$\vec{R} = a\left[\frac{1}{\sqrt{2}}(n_1\hat{i}+n_2\hat{j})+n_3\hat{k}\right]$$

$$\xi_\mu = \frac{1}{8}\sum_{n_1,n_2} \frac{3n_3^2 - \left[\frac{1}{2}(n_1^2+n_2^2)+n_3^2\right]}{\left[\frac{1}{2}(n_1^2+n_2^2)+n_3^2\right]^{\frac{5}{2}}}$$

$$\text{with} \quad \mu = 4n_3 \quad (n_3 = 1,2,...)$$

(5.12)

The even numbered planes are those in common with the FCC structure - the odd numbered planes are the new ones. As in the previous cases, here also $\xi_\mu = \xi_{-\mu}$; we give the values of ξ_μ in Table 1 and some portions of the computer programs are given in appendix IV. Again to the accuracy we are interested, only ξ_0, ξ_1, ξ_2, ξ_3, and ξ_4 (calculated from equation 5.8-12) have non-zero values - the rest of them can be taken to be zero. We note also that $\Sigma_\mu \xi_\mu = -8\pi/3$ (to 0.05 percent) as is to be expected, since diamond structure has cubic symmetry.

To determine the local field near the surface, we consider for this case a 33 layer slab - we take a larger number of layers as now there are more non-zero ξ_μ's and also because, in contrast to the other cases, the influence of the other two planes above and below the reference plane is comparable to the reference plane itself.

The results for the dipole moment density and the dipolar field obtained by inverting the matrix M also show (Fig.5.6) some interesting

results. There is a large range of Γ, from $-0.12(\sim -3/8\pi)$ to very large negative values, for which the inversion process breaks down. We have shown the results for Γ =-0.1 just above this range. We see the behaviour similar to the other cases - both P_μ/P_b and E_μ/E_b are less than one on the surface plane and monotonically goes to one as we go into the bulk. For large positive values of Γ, P_μ/P_b and E_μ/E_b behave in a different manner. We show in figure(5.6), the results for Γ =10. We see that P_μ/P_b has a large oscillatory behaviour. The first layer has a P_μ greater than twice the bulk value - while the second layer has a negative value - i.e. the dipole moment is in the direction opposite that of the bulk ! The dipolar field is also oscillatory - but the dipolar fields for the first and second layers are $0.98E_b$ and $1.01E_b$ - which is quite a contrast to the behaviour for the dipole moments. This can happen, because, as we have remarked above, the influence of the two neighbouring planes together is actually greater than that of the reference plane. The oscillations in P_μ are such that their total effect is to make the dipolar field for each layer remains almost the same. For Γ =0.5, the results shown in figure (5.6), are similar - but now the oscillations in P_μ/P_b are smaller. For values of Γ larger than 10, the oscillations grow larger and at some stage 33 layers are inadequate to achieve convergence. However, for the values of Γ shown in the Fig. 5.6 convergence was achieved with 33 layers. In fig 5.7 we show the polarisation for Γ=-0.18, where our method is not strictly valid, as no convergence can be achieved. It is clear from looking at the figure why convergence cannot be achieved - the almost perfect oscillatory behaviour is a strong indication that for this value of Γ a polarisation wave mode is supported by the system. However, our results for this value of Γ is only indicative, as our method is not formally valid for

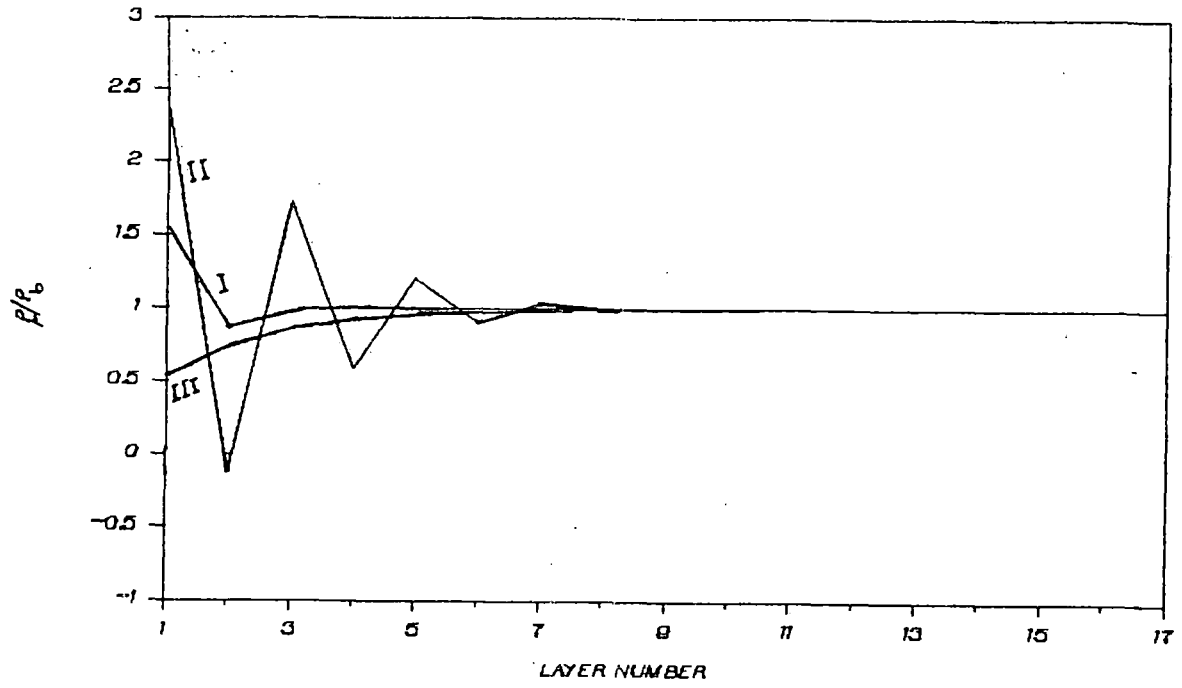

[a]

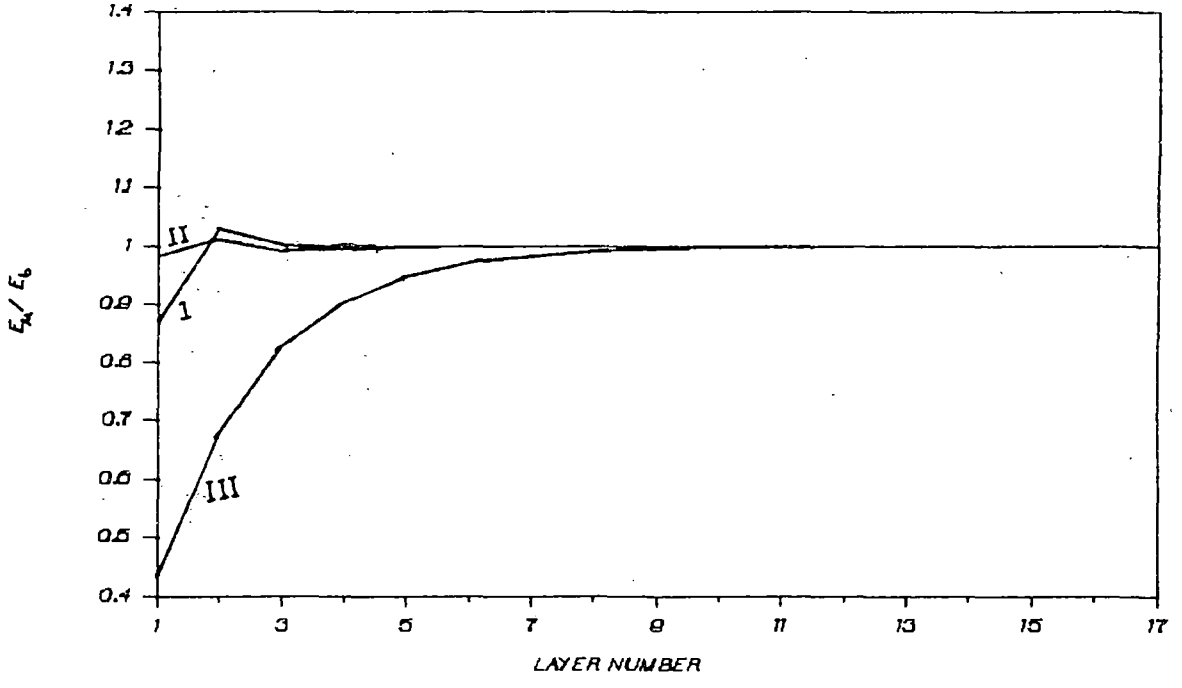

[b]

Fig 5.6 Variation of [a] $P\mu/P_b$ and [b] $E\mu/E_b$ againnst μ for Γ =0.5 (I), 10.0 (II) and −0.1 (III) in diamond structure